IAI
Journals.ASM.org

Analysis of Autoinducer-2 Quorum Sensing in *Yersinia pestis*

Jing Yu,[a] Melissa L. Madsen,[a]* Michael D. Carruthers,[a]* Gregory J. Phillips,[a] Jeffrey S. Kavanaugh,[b] Jeff M. Boyd,[b]* Alexander R. Horswill,[b] F. Chris Minion[a]

Department of Veterinary Microbiology and Preventive Medicine, Iowa State University, Ames, Iowa, USA[a]; Department of Microbiology, Roy J. and Lucille A. Carver College of Medicine, University of Iowa, Iowa City, Iowa, USA[b]

The autoinducer-2 (AI-2) quorum-sensing system has been linked to diverse phenotypes and regulatory changes in pathogenic bacteria. In the present study, we performed a molecular and biochemical characterization of the AI-2 system in *Yersinia pestis*, the causative agent of plague. In strain CO92, the AI-2 signal is produced in a *luxS*-dependent manner, reaching maximal levels of 2.5 μM in the late logarithmic growth phase, and both wild-type and pigmentation (*pgm*) mutant strains made equivalent levels of AI-2. Strain CO92 possesses a chromosomal *lsr* locus encoding factors involved in the binding and import of AI-2, and confirming this assignment, an *lsr* deletion mutant increased extracellular pools of AI-2. To assess the functional role of AI-2 sensing in *Y. pestis*, microarray studies were conducted by comparing Δ*pgm* strain R88 to a Δ*pgm* Δ*luxS* mutant or a quorum-sensing-null Δ*pgm* Δ*ypeIR* Δ*yspIR* Δ*luxS* mutant at 37°C. Our data suggest that AI-2 quorum sensing is associated with metabolic activities and oxidative stress genes that may help *Y. pestis* survive at the host temperature. This was confirmed by observing that the *luxS* mutant was more sensitive to killing by hydrogen peroxide, suggesting a potential requirement for AI-2 in evasion of oxidative damage. We also show that a large number of membrane protein genes are controlled by LuxS, suggesting a role for quorum sensing in membrane modeling. Altogether, this study provides the first global analysis of AI-2 signaling in *Y. pestis* and identifies potential roles for the system in controlling genes important to disease.

Yersinia pestis, the etiologic agent of plague, also called Black Death, has killed over 200 million people throughout recorded history (1). It has two transmission routes: the most common is through flea bites, and the other is via airborne droplets. The lifestyle of *Y. pestis* is complex and involves two distinct environments, the flea midgut and mammalian hosts (2). The distinct environments in which *Y. pestis* must survive require complex gene regulatory mechanisms to conserve energy. Gene regulation in *Y. pestis* is also responsive to temperature shifts between the ambient temperature of the flea vector and the temperature of the human host (3), complicating the regulatory circuits and data analysis.

Quorum sensing (QS) is a process of cell-to-cell communication that relies upon secretion and detection of chemical signals called autoinducers (AIs). *Yersinia pestis* possess two conserved QS systems, the AI-1 pathway, which utilizes acyl homoserine lactones (AHLs) as signals, and the LuxS pathway, which responds to AI-2 (4). The AI-2 signaling pathway is common to many bacteria through homologues of the *luxS* gene. LuxS generally has two functions: one is to generate the major methyl donor *S*-adenosylmethionine, and the other is to detoxify *S*-adenosyl-L-homocysteine to homocysteine and 4,5-dihydroxy-2,3-pentandione (DPD). DPD undergoes further cyclization rearrangements to yield AI-2 (5). AI-2 is derived from the ribose moiety *S*-ribosylhomocysteine (SRH). It has been proposed to serve as a universal signaling molecule for interspecies communication (5). In *Escherichia coli* and *Salmonella*, the AI-2 signal is the ligand for a periplasmic protein LuxP homologue (LsrB) and is detected by the ATP binding cassette (ABC) transporter/receptor on the cell membrane. AI-2 internalization is dependent on the Lsr transporter (*luxS* regulated). The *lsr* operon contains seven genes in the organization *lsrACDBEFGR*, and its transcription is induced by the presence of AI-2. The four promoter-proximal genes *lsrACDB* encode the components of the AI-2 importer (6). The *lsrR* gene encodes a repressor of the *lsr* operon but is a pseudogene in *Y. pestis*, suggesting that AI-2 synthesis is constitutive in this species.

Whether or not AI-2 quorum sensing is crucial for *Y. pestis* pathogenesis is unclear. While there is some evidence that mice challenged with a *luxS*::*kan* mutant did not show a loss of virulence, as determined by the 50% lethal dose (LD_{50})(4), an in-depth analysis of the role that QS, via AI-2, plays in controlling the expression of virulence genes has not been performed. Specifically, the number and types of genes controlled by QS have not been studied systematically. To obtain a better understanding of the role of AI-2 quorum sensing in *Y. pestis*, we performed transcriptional profiling experiments to identify AI-2 QS-regulated genes and networks at 37°C, representing the mammalian host temperature. Our results indicated that AI-2/LuxS quorum sensing is important for *Y. pestis* adaptation and survival in diverse environments, including oxidative stress.

MATERIALS AND METHODS

Bacterial strains and culture conditions. The strains and plasmids used in this study are described in Table 1. *Yersinia pestis* strains were derived

Received 6 August 2013 Accepted 7 August 2013
Published ahead of print 19 August 2013
Editor: A. J. Bäumler

Address correspondence to F. Chris Minion, fcminion@iastate.edu.

* Present address: Melissa L. Madsen, CEVA Biomune, Lenexa, Kansas, USA; Michael D. Carruthers, Center for Microbial Pathogenesis, The Research Institute at Nationwide Children's Hospital, Columbus, Ohio, USA; Jeff M. Boyd, Department of Biochemistry and Microbiology, Rutgers University, New Brunswick, New Jersey, USA.

Supplemental material for this article may be found at http://dx.doi.org/10.1128/IAI.00880-13.

doi:10.1128/IAI.00880-13

TABLE 1 Bacterial strains used in this study

Strain or plasmid	Genotype or description	Reference or source
Strains		
Escherichia coli		
BW25141	Cloning strain	9
ER2566	Overexpression strain	New England Biolabs
AH-pfs	ER2566/pET28a-*pfs* (Kan^r)	This work
AH-luxS	ER2566/pET28a-*luxS* (Kan^r)	This work
AH1070	ER2566/pET28a-*lsrB* (Kan^r)	This work
Yersinia pestis		
CO92	*Yersinia pestis* Lcr$^+$ Pgm$^+$	7
R88	CO92 Lcr$^+$ Δ*pgm*	R. D. Perry
R115	CO92 Lcr$^+$ Δ*pgm* Δ*ypeIR* Δ*yspIR* Δ*luxS*::*kan*	R. D. Perry
ISM1980	R88 Δ*luxS*::*kan*	This work
YP21	R88 Δ*luxS*::*kan*	This work
YP23	R88 Δ*luxS*::*frt*/pJET1.2 (Amp^r)	This work
YP21	R88 Δ*luxS*::*frt*/pJET1.2-*luxS*	This work
YP24	R88 Δ*lsr*::*frt*	This work
Vibrio harveyi MM32	*luxN*::*cat luxS*::Tn*5kan*	12
Plasmids		
pET28a	Overexpression vector (Kan^r)	Novagen
pET28a-*pfs*	Pfs expression vector (Kan^r)	This work
pET28a-*luxS*	LuxS expression vector (Kan^r)	This work
pET28a-*lsrB*	LsrB(Δ2–25) expression vector (Kan^r)	This work
pJET1.2	Cloning vector (Amp^r)	Fermentas
pJET1.2-*luxS*	*luxS* complementation vector (Amp^r)	This work

from a *pgm* deletion mutant of strain CO92 (7) and maintained in brain heart infusion (BHI) broth. For all microarray experiments, *Y. pestis* strains were grown overnight in BHI broth at 30°C. These cultures grown overnight were diluted 1:100 into fresh BHI culture medium supplemented with 2.5 mM calcium chloride and incubated at 37°C until the cell density reached an optical density at 600 nm (OD_{600}) of 1.0, about 9 to 10 h. This was an optical density at which the culture demonstrated maximum induction of AI-2 under the conditions tested (Fig. 1). Cell growth was monitored on a Bausch and Lomb Spectronic 20 spectrophotometer at a wavelength of 600 nm. For experiments measuring AI-2 production, *Y. pestis* cells from glycerol stocks stored at −80°C were streaked onto BHI slants containing appropriate antibiotics and grown at 30°C for approximately 24 h. Cells were washed off slants by using 5 ml BHI broth containing appropriate antibiotics, and these cultures were grown overnight (~12 h) at 30°C with shaking. The cultures grown overnight were then used to inoculate fresh BHI broth at a 1:500 dilution. *Escherichia coli* strains were maintained in Luria-Bertani (LB) broth, and *Vibrio harveyi* cells were maintained in autoinducer bioassay (AB) medium (8). Antibiotic concentrations (in μg/ml) used in bacterial cultures were as follows: 50 μg/ml kanamycin (Kan), 10 μg/ml chloramphenicol (Cam), and 100 μg/ml ampicillin (Amp). All reagents were purchased from Fisher Scientific (Pittsburg, PA) or Sigma (St. Louis, MO), unless otherwise indicated.

Strain construction. The *Y. pestis* Δ*luxS*::*frt* mutant (strain YP21) was constructed by bacteriophage lambda Red-mediated recombination. Briefly, a Cam^r antibiotic resistance cassette was amplified from pKD3 (9) by using oligonucleotides YpluxS-S and YpluxS-AS (Tables 2 and 3). Purified PCR products were electroporated into strain R88 carrying plasmid pRedET (10). Individual Cam^r colonies were selected at room temperature and cultured at 37°C to screen for the loss of pRedET. The Cam^r cassette was subsequently removed by site-specific recombination by transformation with pCP20, as described previously (9). A similar *luxS* knockout mutation in R88 was also constructed with a Kan^r marker by using pKD4 (9) as the template with the same primers, creating strain ISM1980.

A *luxS* complementation plasmid was constructed by amplifying the *luxS* gene using primers Yp-luxS.S and Yp-luxS.AS. The PCR product (~0.8 kbp) was gel purified, blunt ended, and cloned into the vector pJET by using the CloneJET PCR cloning kit (Fermentas). A *luxS* overexpression plasmid was constructed by amplifying the *luxS* gene by PCR using oligonucleotides forluxS and revluxS (Tables 2 and 3). The PCR product was digested with NheI and HindIII and ligated into pET28a (Novagen) cut with the same enzymes. A *pfs* overexpression plasmid was constructed by amplifying the *pfs* gene by PCR using oligonucleotides forpfs and revpfs (Tables 2 and 3). The PCR product was digested with NdeI and BamHI and cloned into pET28a cut with the same enzymes.

In a similar fashion, a *Y. pestis* Δ*lsr*::*kan* operon deletion (strain YP26) was constructed. Oligonucleotides YplsrA2-ko.S and Yplsr-ko.AS were used to amplify a Kan^r cassette from pKD4 (9). Purified PCR products were electroporated into R88 carrying plasmid pRedET, and Δ*lsr*::*kan* mutants were isolated as described above.

Pfs and LuxS purification. Plasmid pET28a-*pfs* or pET28a-*luxS* was then transformed into *E. coli* expression strain ER2566 by electroporation. For purification of either protein, the expression strain was grown over-

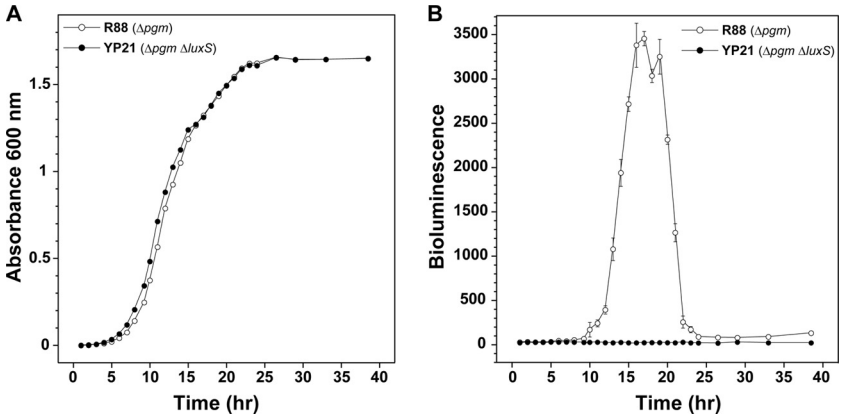

FIG 1 Growth and AI-2 production in *Y. pestis* strain R88 (Δ*pgm*) and the Δ*luxS* mutant. (A) Growth of strains with shaking in BHI broth at 30°C. (B) At each time point during growth, cell supernatants were collected, filtered, and assayed for AI-2 by using the *V. harveyi* MM32 reporter strain (see Materials and Methods). Data represent the means of two *Y. pestis* cultures per strain (A) and means ± standard deviations of four wells of MM32 medium per time point for two experiments ($n = 8$) (B).

TABLE 2 Primers used for cloning

Primer	Sequence[a]
YpluxS-S	ATGCCATTATTGGATAGCTTTACCGTAGACCATACCATTATGAAAGCAGTGTAGGCTGGAGCTGCTTC
YpluxS-AS	AATATGCAATTCAGTCAGTTTCTCTTTCGGCAGTGCCAACTCTTCGTTCATATGAATATCCTCCTTAG
YplsrA2-ko.S	AGAGGCAAGGAGCCTTCCAAAGAGACGTCGTCAACCCACAATCCATGTGTAGGCTGGAGCTGCTTCG
Yplsr-ko.AS	CTAAGGCATTAGGCCGATAAATACCGTTTTTTTGCGTGGCCCCGTCATATGAATATCCTCCTTAG
Yp-luxS.S	GAGTATTTAGCGCTTCATGGTGGC
Yp-luxS.AS	ACTGACCCAAAGCTGAAAGC
forluxS	GTTGTTGCTAGCATGCCATTATTGGATAGCTTTACCG
revluxS	GTTGTTAAGCTTCTAAATATGCAATTCAGTCAGTTTCTC
forpfs	CAGCGAGTATCCATATGAAAGTAGG
revpfs	GTTGTTGGATCCCATCATTAACCGCGTTGCGCC

[a] Underlined sequences are restriction sites included for cloning purposes.

night and inoculated at a dilution of 1:200 into 2 liters of LB broth supplemented with Kan. Cultures were grown at 37°C to an OD_{600} of ~0.6, and gene expression of the protein of interest was induced with 1 mM isopropyl-β-D-thiogalactopyranoside. After 2 h under inducing conditions, cells were harvested by centrifugation at 6,000 × *g* for 10 min and suspended in 25 ml of ice-cold equilibration buffer (0.5 M NaCl, 5 mM imidazole, and 20 mM Tris [pH 7.9]). Cells were lysed with 3 ml of 10× BugBuster (Novagen) on a nutating mixer at 4°C for 2 h. Insoluble debris was removed by centrifugation at 30,000 × *g* for 35 min, and the cleared cell lysates were loaded onto 5-ml columns containing His-Select resin (Sigma) equilibrated at room temperature with equilibration buffer. The columns were washed with 30 ml of equilibration buffer followed by 50 ml of wash buffer (0.5 M NaCl, 60 mM imidazole, and 20 mM Tris [pH 7.9]), and the Pfs and LuxS proteins were then eluted with 50 ml of elution buffer (0.5 M NaCl, 1 M imidazole, 20 mM Tris [pH 7.9]). Fractions containing Pfs and LuxS proteins were identified by SDS-PAGE. Pooled fractions were concentrated by using 10-kDa-cutoff Amicon Ultra centrifugal filters (Millipore) and dialyzed against 10 mM Tris (pH 7.5) by using 10-kDa-cutoff Slide-A-Lyzer cassettes (Pierce). The protein concentration of the purified enzymes was determined by a Bradford assay (Bio-Rad), and glycerol was added to a final concentration of 33% before the Pfs and LuxS proteins were flash frozen at concentrations of 23 mg/ml and 28 mg/ml, respectively, by dripping the protein solutions into liquid nitrogen. Frozen pellets of Pfs and LuxS were stored at −80°C until they were used for biosynthesis of AI-2.

AI-2 biosynthesis. AI-2 was biosynthesized from *S*-adenosylhomocysteine (SAH) in a two-step enzymatic process that used purified *Y. pestis* Pfs and LuxS enzymes, which was analogous to that described previously for the *in vitro* synthesis of AI-2 using purified *Vibrio harveyi* enzymes (11). In the first reaction, SAH was converted to *S*-ribosylhomocysteine (SRH) and adenine by the enzymatic action of Pfs. Specifically, 10 mM SAH in 50 μl of 50 mM Tris-HCl (pH 7.5) was incubated at 25°C with 4.2 μM purified *Y. pestis* Pfs (see the description of Pfs purification above). The reaction progress was monitored by measuring the time-dependent decrease in absorbance at 276 nm, which is due to adenine having a lower extinction coefficient than adenosine, and was found to be complete within 1 h. After 4 h of incubation, the Pfs reaction mixture was passed through an Amicon Ultra centrifugal filter device with a 5-kDa cutoff (Millipore) in order to remove the Pfs enzyme. In the second step of biosynthesis, *S*-ribosylhomocysteine produced by the Pfs reaction was enzymatically converted by LuxS to homocysteine and 4,5-dihydroxy-2,3-pentanedione (DPD), which spontaneously cyclizes to form bioactive AI-2. This was accomplished by adding purified *Y. pestis* LuxS (see the description of LuxS purification above) to the filtered Pfs reaction mixture at a concentration of 2.5 mg/ml and allowing the mixture to incubate at room temperature for up to 24 h. Production of DPD was monitored indirectly by periodically determining the concentration of homocysteine by using Ellman's reagent [5,5′-dithiobis-(2-nitrobenzoic acid) (DTNB)], since the LuxS reaction produces equimolar quantities of DPD and homocysteine. Specifically, 15 μl of the LuxS reaction mixture was removed periodically and mixed with 985 μl of 100 μM DTNB in 100 mM Tris (pH 8.0), and the absorption at 412 nm was measured and converted to a molar concentration by using an extinction coefficient of 14,150 M^{-1} cm^{-1}. LuxS was removed from the reaction mixture by passage through an Amicon Ultra centrifugal filter device with a 5-kDa cutoff, and aliquots were frozen and stored at −20°C until they were used for bioluminescent or microarray assays.

***V. harveyi* AI-2 bioassay.** For all experiments measuring growth-dependent production of AI-2 by *Y. pestis*, the cultures were grown overnight, as described above, by using the following procedure. Cells were diluted 1:500 in 5 ml of fresh BHI broth and grown at 30°C with shaking for ~20 h. This culture was diluted 1:1,000 in 50 ml of fresh BHI broth, and AI-2 production was measured. At the indicated time points, 1 ml of culture was removed, the OD_{600} was measured by using a Tremo Spectronic Genesys 20 spectrophotometer, and 600 μl (of the 1 ml) was sterilized by using 0.22-μm Costar Spin-X centrifuge tube filters (Corning). The sterile conditioned medium was diluted 1:10 and 1:100 with BHI broth (1 ml was prepared for each dilution), and all tubes were frozen and stored at −80°C until the AI-2 concentration was measured.

AI-2 concentrations were measured by using *V. harveyi* reporter strain MM32 (12). This strain will produce light only when AI-2 is supplied

TABLE 3 Primers used for quantitative RT-PCR

Gene	Primer sequence	
	Forward	Reverse
aceA	AGATGTCTTGGGTGTACCAACGCT	AGCAGTACGGTCGCCGGTAATAAA
agaZ	GTGCAGCCTGGTGTTGAGTTTGAT	AATCGGTGGAGTGGGCTTCGAATA
caf1	AACTTTACAGATGCCGCGGGTGAT	AGCGAACAAAGAAATCCTGGCTGC
deoB	ATCTGCCGGGCTATTTGGGTAACT	GGGCAATTTCGCACAGCTCATACA
fruK	GATCAACGTTGCCAAGGTGCTGAA	AGTCACTTCGCCATCTTTCTCGGT
galT	CAATCGCCCATGCTGCTGGATTAT	TAAGGCACTACCGCTAGCCAATGT
gltP	ATGCGAAGAAACTTGGCCGGATTG	TCAACGACGGTTAGCGCAGACATA
katY	ACCGATGTCAGTTCTTTCGCGGTA	TCAGGCACGGTCAGTTCCAGTTTA

exogenously, since it contains deletions of *luxN* and *luxS* (Table 1) that render it incapable of sensing homoserine lactones or synthesizing AI-2. For measurement of AI-2 concentrations, a culture of MM32 grown overnight in AB medium was used to inoculate fresh AB medium at a 1:500 dilution. After ~1 h of growth at 30°C with shaking, 180-μl aliquots of the MM32 culture were transferred onto 96-well microtiter plates (Costar 3603), to which 20 μl of *Y. pestis* conditioned medium (4 wells per dilution per time point) had already been added. After mixing, the final dilutions of the conditioned medium relative to the *Y. pestis* culture were 1:10, 1:100, and 1:1,000. The microtiter plates were incubated at 30°C with shaking, and at 2-h intervals (for 10 h), the OD_{600} and luminescence were measured by using either a Tecan GENios or a Tecan Infinite 200 M microtiter plate reader. The luminescence values and AI-2 concentrations reported are those measured after 6 h of MM32 growth.

AI-2-induced luminescence by MM32 was converted to a molar concentration by developing a standard curve using known signal concentrations of biosynthesized AI-2. The standard curve was made by using the same MM32 culture used to measure AI-2 in conditioned medium, and OD and luminescence measurements were taken at the same time points in order to minimize differences. Luminescence values, measured at 6 h of MM32 growth, were normalized to OD_{595} values and plotted versus the AI-2 concentration. The resulting plot of OD-normalized luminescence versus AI-2 concentration was fit to a 5-parameter logistic fit by using KaleidaGraph software (Synergy Software). The resulting standard curve was used to convert OD-normalized luminescence values measured for *Y. pestis* conditioned medium to molar AI-2 concentrations.

AI-2 levels in virulent *Y. pestis* CO92 cells. Virulent strain *Y. pestis* CO92 was obtained from the Biodefense and Emerging Infections Research Resources Repository. The strain was maintained and grown in the biosafety level 3 (BSL-3) facility at the Department of Veterinary Microbiology and Preventive Medicine, Iowa State University, according to established protocols. For the AI-2 time course, strain CO92 was grown in BHI in a similar manner as described above. Spent medium was collected at the indicated time points, sterilized by using a 0.22-μm filter, and confirmed as being culture negative. Samples were saved and tested for AI-2 as described above.

Microarray experimental design. For each microarray experiment, the transcriptomes of the *luxS* mutant (ISM1980) or the *luxS yspIR ypeIR* triple mutant (R115) were compared with that of the CO92 Δ*pgm* isogenic parent strain R88. In these experiments, the cells were harvested at mid- to late log phase (OD_{600} = 1.0), which was the time when cultures exhibited the greatest amount of AI-2 production (Fig. 1). Two additional experiments were performed with the Δ*pgm* background strain, in which cells were treated with purified QS signals at an early stage of growth prior to the cells achieving quorum sensing (Fig. 1) (13). In one experiment, AI-2 signal, prepared as described above, was added to cultures. In the second experiment, AI-2 plus the two acyl homoserine lactones (AHLs) produced and used by *Y. pestis* [*N*-hexanoyl-DL-homoserine lactone and *N*-(3-oxooctanoyl)-L-homoserine lactone] (Sigma) were added simultaneously. Cultures grown overnight were washed three times to remove any quorum-sensing signals and diluted 1:100 in BHI broth. After 2 h of incubation at 37°C to establish early-log-phase growth, either single AI-2 (500 nM final concentration) or three-signal AI-2 (500 nM final concentration) and AHLs (both at 5 μM final concentrations) were added. The cells were incubated for 4 h at 37°C and then isolated by centrifugation, RNA Protect reagent (Invitrogen) was added, and the cells were stored at −70°C until the RNA was isolated. The control was an identical aliquot of cells from the same culture without added QS signals.

For each experiment, labeled cDNAs generated from RNA from six mutant cultures (biological replicates) were paired with controls for hybridization on a two-color microarray slide. Cy3 and Cy5 dyes were used as labels, and dye assignments for control and mutant samples were reversed for three of the arrays to account for variation in labeling efficiencies (dye bias). Table 4 describes the microarray experiments performed in this study.

TABLE 4 Numbers of significantly regulated genes by different transcriptional studies

Microarray design	No. of significantly regulated genes at a *P* value of <0.05[a]	GEO accession no.
R88 vs *luxS*::*kan*	615	GSE22849
R88 vs Δ*ypeIR* Δ*yspIR luxS*::*kan*	194	GSE21911
Δ*pgm* untreated vs AI-2 treated	32	GSE22848
Δ*pgm* untreated vs AI-2 plus AHL treated	30	GSE22846

[a] All with a fold change of >1.5.

RNA extraction, cDNA synthesis, and labeling. The cells from each culture were collected and were treated with RNA Protect bacterial reagent (Qiagen) and stored at −70°C. RNA was extracted from frozen cell pellets by using the RNeasy minikit (Qiagen) according to the manufacturer's protocol. The RNAs were treated with DNase I (Ambion) for 30 min at 37°C to remove contaminating genomic DNA. PCR was used to confirm DNA removal. The RNAs were then centrifuged through Microcon Ultracel/YM30 filters (Millipore). Ten micrograms of total RNA from each sample was used to synthesize aminoallyl-labeled cDNA by using SuperScript III reverse transcriptase (Invitrogen) and 10 μg of random hexamers (Integrated DNA Technologies). Fluorescently labeled targets were prepared as described previously (14). The frequency of dye incorporation and yield were determined by spectrophotometry (ND-1000; Nanodrop).

Hybridization. Microarray slides were prewashed in water for 5 min and rinsed twice with water for 1 min. Corresponding equal amounts of dye-labeled cDNA targets (1.5 μg) were mixed together, dried, resuspended in 225 μl Long Oligo hybridization solution (Corning), incubated at 95°C for 5 min, and centrifuged for 4 min at 10,000 rpm. This solution was then injected into a Lucidea Slidepro (Amersham Biosciences, Piscataway, NJ) hybridization station containing the prewashed microarray slides. The hybridization lasted for 16 h at 42°C, and the slides were then washed in a series of wash buffers (2× SSC [1× SSC is 0.15 M NaCl plus 0.015 M sodium citrate], 0.1% SDS, 1× SSC, and 0.1× SSC) by the hybridization station and dried by centrifugation at 1,500 × *g* for 30 s.

To enhance the discovery of differentially expressed genes, the hybridized arrays were scanned three times with various laser power and photomultiplier tube values by using a ScanArray HT scanner (PerkinElmer) to detect excited wavelengths, as described previously (15). Image processing and normalization were performed as described previously (15). The normalized values for triplicate spots were averaged within each array to produce one normalized measure of expression of fluorescence for each probe sequence. A mixed-model analysis was conducted as previously described (14).

Real-time RT-PCR. The SensiMix SYBR No-Rox One-Step kit (Bioline) was used to perform the real-time reverse transcription-PCR (RT-PCR) assay on the Mx3005P QPCR system (Stratagene). The quantification cycle (*Cq*) values were exported from MxPro 4.1 software. Three biological *Y. pestis* replicates were used, and all original RNAs were equally diluted to 4 ng/μl. Each RNA template was then diluted 3 times, as described previously for the PREXCEL-Q software program (16). The *leuB* gene was used as the internal reference gene because it showed no transcriptional changes by microarray under any of the experimental conditions. The final reaction mixture volume for each well was 15 μl and contained 7.5 μl SensiMix SYBR No-Rox One-Step, 0.6 μl of each primer at 2.5 μM, 0. 3 μl of 10 U/μl RiboSafe RNase inhibitor, 5 μl RNA, and 1 μl diethyl pyrocarbonate (DEPC)-water. The thermal cycling conditions included a reverse transcription step at 50°C for 30 min; a polymerase activation step at 95°C for 10 min; 40 PCR cycles of 95°C for 30 s, 60°C for 30 s, and 72°C for 30 s; and a melting-curve step of 95°C for 1 min, 55°C for

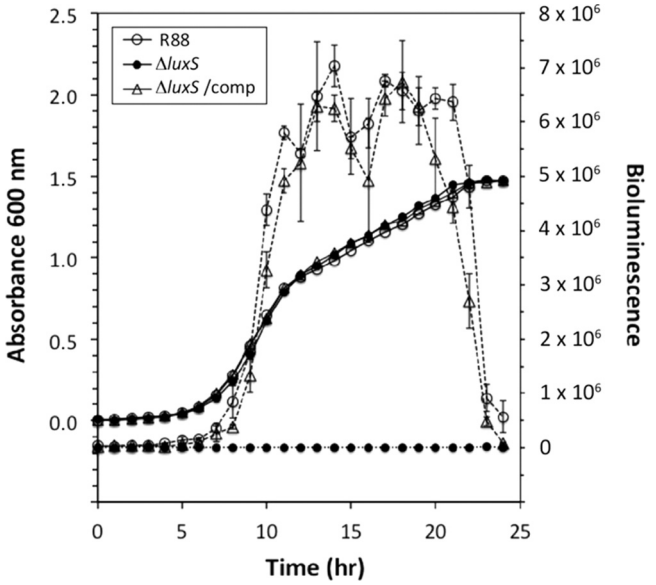

FIG 2 Complementation of the Δ*luxS* mutant. *Yersinia pestis* strain R88, the Δ*luxS* mutant, and the complemented strain were grown with shaking in BHI broth at 30°C. At each time point during growth, cell supernatants were collected, filtered, and assayed for AI-2 by using the *V. harveyi* MM32 reporter strain. Data represent the means ± standard deviations of triplicate wells per time point and strain.

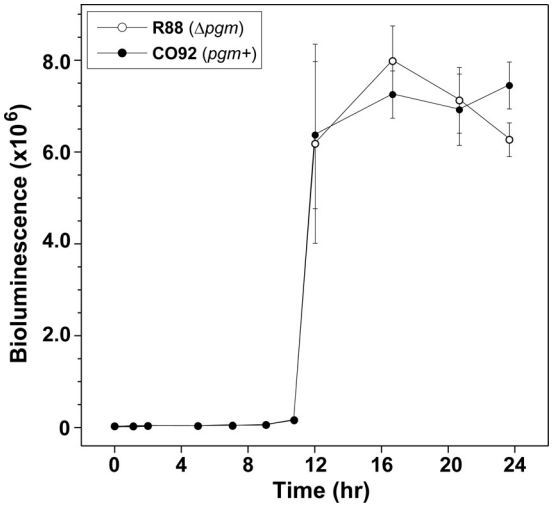

FIG 3 Comparison of AI-2 production in *Y. pestis* wild-type strain CO92 and strain R88 (Δ*pgm*). *Yersinia pestis* strain R88 and wild-type strain CO92 were grown with shaking in BHI broth at 30°C in a BSL-3 facility. At each time point during growth, cell supernatants were collected, filtered, and assayed for AI-2 by using the *V. harveyi* MM32 reporter strain. Data represent the means ± standard deviations of triplicate wells per time point.

30 s, and 95°C for 30 s. The data were analyzed according to methods described previously by Gallup and Ackermann (16).

Hydrogen peroxide killing assays. Strains R88 and YP21 (Δ*luxS*::Cm) were grown as 5-ml cultures overnight in BHI broth at 37°C with 4 mM $CaCl_2$ supplementation to an OD_{600} of 3 to 4. Cells were pelleted by centrifugation, the growth medium was decanted, and the cell pellet was suspended in an equal volume of 10 mM phosphate-buffered saline. Strains were diluted to an OD_{600} of 0.25 in a 1-ml total volume in 15-ml culture tubes. After treatment with different concentrations of hydrogen peroxide for 1 h, 50 μl of the cell suspension was diluted into 1 ml in PBS with 1 mg/ml catalase (Sigma) to quench the reaction. The samples were further serially diluted, spotted onto BHI agar plates, and grown at 30°C to determine the CFU per ml.

Microarray data accession numbers. The microarrays used in these studies can be found in the National Center for Biological Informatics Gene Expression Omnibus (GEO) under platform accession numbers GPL9009 and GPL10017. All microarray data are available under the GEO accession numbers given Table 4.

RESULTS

LuxS-dependent production of AI-2. To initiate studies on AI-2 signaling, the *luxS* gene was deleted from the Δ*pgm* mutant of CO92 (strain R88) by using lambda Red recombinase, resulting in strain YP21 (Table 1). No growth defects in YP21 were observed compared to the parent during growth at 30°C in rich medium (Fig. 1A). For monitoring AI-2 production, *Vibrio harveyi* reporter strain MM32 was utilized throughout this report. MM32 is unable to synthesize AI-2 due to a *luxS* mutation, and additionally, the presence of a *luxN* mutation strain blocks the bioluminescent response to AI-1 (12). Thus, MM32 will bioluminesce only in the presence of exogenously added AI-2, making it a robust and more sensitive AI-2 reporter than the commonly used strain BB170. The bioluminescent response of MM32 was confirmed through control experiments using culture supernatants from known producers of AI-2 (data not shown).

To generate a profile of AI-2 production in *Y. pestis*, the levels of AI-2 were monitored over time in R88 and its isogenic Δ*luxS* knockout. Cultures were grown at 30°C in rich medium, and cell-free supernatants were assayed for AI-2 by using the MM32 reporter strain. The R88 strain produced robust levels of AI-2 during an approximately 10-h window in late logarithmic phase (Fig. 1B). As anticipated, deletion of *luxS* in YP21 eliminated AI-2 production. As the cells entered stationary phase, the extracellular AI-2 concentration in R88 dropped off dramatically to almost undetectable levels. To confirm the role of LuxS, a plasmid containing the *luxS* gene and its native promoter were transformed into YP21 to create strain YP24. Compared to the empty vector control (strain YP23), the *luxS* plasmid complemented AI-2 production to levels similar to those of strain R88 (Fig. 2), indicating that the lack of AI-2 production was not due to secondary mutations. These findings demonstrate that the LuxS enzyme is essential for *Y. pestis* AI-2 production during late logarithmic growth.

Δ*pgm* mutation does not affect AI-2 production. The Δ*pgm* mutation in *Y. pestis* strain R88 removes 102 kb of chromosomal DNA, resulting in attenuation (17). Since this deletion is large and encompasses many genes, it was important to assess the contribution of this mutation to AI-2 production. For this comparison, a time course experiment was performed to measure the expression of extracellular levels of AI-2 produced by wild-type CO92 and strain R88. Overall, the Δ*pgm* mutation had no observable effect on AI-2 production, as near-identical AI-2 production was observed between the two strains (Fig. 3). Throughout the rest of this report, all studies were performed with Δ*pgm* mutant strain R88.

The *lsr* chromosomal region. Genetic and molecular studies of *Salmonella enterica* have revealed that AI-2 signaling occurs through a different mechanism than that in the *V. harveyi* paradigm model. Central to the difference is the presence of the *lsr* chromosomal locus, encoding factors necessary for AI-2 binding, import, and intracellular regulation (18, 19). Our bioinformatic analysis of the CO92 chromosome indicates the presence of a gene

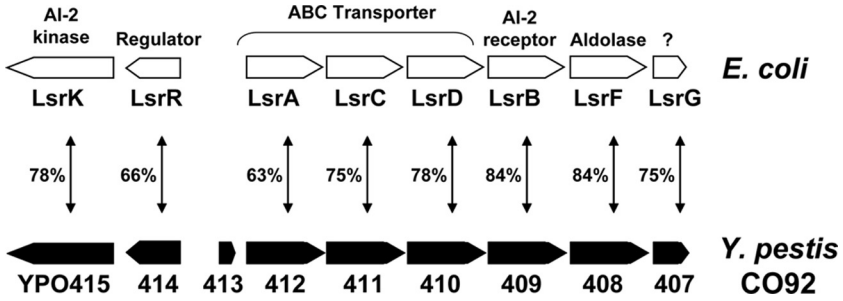

FIG 4 The *lsr* region of *Y. pestis* CO92 compared to that of *E. coli*. The CO92 open reading frame designations (YPO407 to YPO415) are shown on the bottom of the schematic. The percent identity of the CO92-encoded proteins with the corresponding *E. coli* Lsr proteins is indicated. An additional open reading frame, YPO413, is present in the intergenic region of the CO92 genome.

cluster with striking similarity to the *S. enterica* and *E. coli lsr* loci. Other research groups have made similar claims about the presence of a potential *lsr* locus in *Y. pestis* through sequence analysis (20, 21).

The cluster stretches from *Y. pestis* CO92 open reading frames (ORFs) YPO415 through YPO407 (Fig. 4). ORFs YPO414 and YPO415 encode proteins with similarity to the LsrR transcriptional regulator and LsrK AI-2 kinase, respectively. In the intergenic region, there is a short gene, called YPO413, that does not exist in other enteric *lsr* regions. Divergently transcribed from the predicted LsrR regulator, ORFs YPO412 through YPO410 share similarity with the ABC transporter LsrACD, while YPO409 is similar to the periplasmic receptor called LsrB. Finally, the YPO408 and YPO407 ORFs share similarity to the LsrF and LsrG enzymes, respectively.

We hypothesized that mutations in the *lsr* locus would alter the extracellular level of AI-2 over time. To investigate this question, a complete deletion of the locus was constructed by lambda Red recombination. The time course to monitor AI-2 production was performed similarly to that for *luxS* mutant strain YP26. Similar levels of AI-2 were detected in the spent media of YP26 and the parent strain R88 during logarithmic growth (Fig. 5A). Interestingly, the extracellular level of AI-2 remained high in YO26 as it entered stationary phase, while the level of AI-2 in R88 dropped off dramatically.

To quantify the difference between YP26 and R88, a bioassay standard curve was generated by using biosynthesized AI-2 (Fig. 5B). AI-2 was obtained by overexpressing and affinity purifying the *Y. pestis* CO92 Pfs and LuxS enzymes and performing a two-step conversion of *S*-adenosylhomocysteine to DPD, as described in Materials and Methods. By extrapolation to the standard curve, the AI-2 concentration was determined throughout the time course (Fig. 5C). In both strains R88 and YP26, peak production of AI-2 reached levels of ~2.5 μM in the late logarithmic growth phase. In stationary phase, the AI-2 levels dropped to 0.2 μM by 25 h of growth and remained fairly constant in the 0.2 to 0.3 μM range. In contrast, the AI-2 levels in YP26 ranged from 1.1 to 1.4 μM in stationary phase but eventually dropped to under 1 μM at later time points (Fig. 5C). Altogether, YP26 showed no defect in AI-2 production, but the mutant displayed an altered phenotype in the stationary-phase levels of the signal. Thus, these findings implicate the *Y. pestis lsr* chromosomal region in stationary-phase degradation or transport of the AI-2 signal.

Effect of QS pathways on gene expression. To obtain a better understanding of the role of LuxS, Ype, and Ysp pathways at the mammalian host temperature, we measured transcript levels in

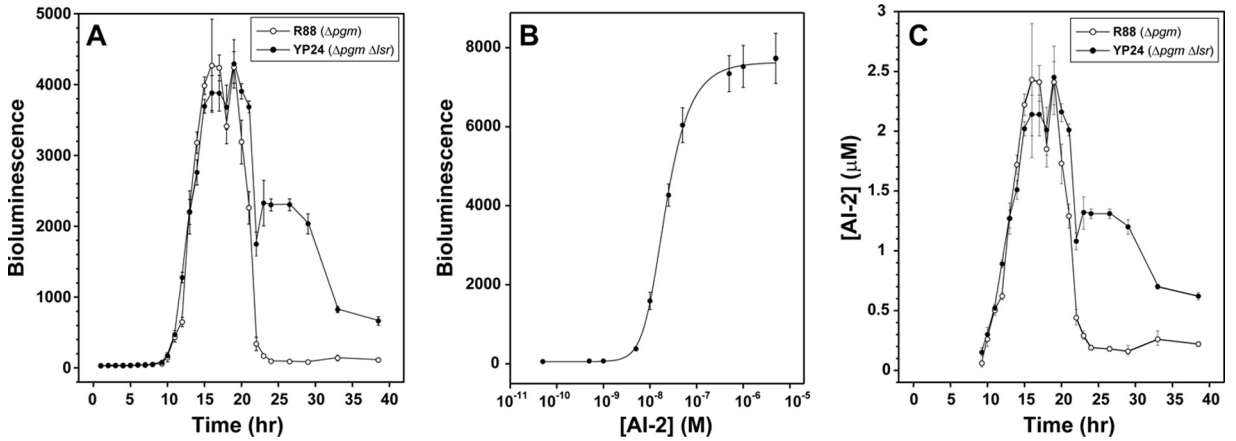

FIG 5 AI-2 production profile of the *Y. pestis* Δ*lsr* mutant and quantification of signal levels. (A) *Yersinia pestis* strain R88 and the Δ*lsr* mutant were grown with shaking in BHI broth at 30°C. At each time point during growth, cell supernatants were collected, filtered, and assayed for AI-2 by using the *V. harveyi* MM32 reporter strain. (B) AI-2 was biosynthesized by using purified *Y. pestis* CO92 Pfs and LuxS enzymes (see Materials and Methods). A standard curve was prepared by using synthesized AI-2 in the *V. harveyi* bioassay. (C) Conversion of the bioluminescence output into AI-2 concentrations by using the developed standard curve. Data represent the means of two cultures per *Y. pestis* strain (A), means ± standard deviations of two cultures with 4 wells per time point (B), and the same data as in panel A with bioluminescence converted to μM by using the curve in panel B (C).

R88 and compared them to the levels in triple mutant strain R115, as described above. In this experiment, 194 genes were found to be differentially expressed at least 1.5-fold ($P < 0.05$), and 92 genes were differentially expressed with a P value of <0.01 (see Table S1 in the supplemental material). Genes upregulated in response to all three QS systems with the highest fold changes included *lsrK* (YPO0415) (kinase that phosphorylates carbon-5 of the open form of DPD), *lamB* and *malMKEFG* (maltose transport and metabolism), *agaYZ* (tagatose metabolism), *gltA* and *icdA* (Krebs cycle), *tcaA* (insecticidal toxin), *yapM* (YPO0823) (autotransporter), and *metA* (homoserine *O*-succinyltransferase). Genes downregulated in response to all three QS systems included *yopEPT* (effector proteins), *sycEN* (Yop chaperones), and *yscABCDEFGHIJKLMNOPQRSTXY* and *lcrDF* (low-calcium response).

***luxS*-regulated genes.** To clarify the role of the *luxS* gene at the host temperature, we measured transcript levels in ISM1980 and compared them to the transcript levels in R88 at 37°C, as described above. In this experiment, 615 genes were found to be differentially expressed at least 1.5-fold at a P value of <0.05, and 220 genes were differentially expressed at a P value of $P<0.01$ (see Table S2 in the supplemental material). Genes upregulated in response to AI-2 included the *lsr* operon (*lsrABCDGFKR*) (AI-2 regulation), *mglBC* and *galEKT* (monosaccharide galactose uptake and metabolism), *lamB* and *malMKEFGSZ* (maltose metabolism), *aceABK* (glyoxylate bypass), *acs* (acetyl coenzyme A synthetase), *araFGH* (arabinose operon), *deoB* (phosphopentomutase), *gcsH* and *gcvPT* (glycine degradation), *yfiA* (putative σ^{54} modulation protein), *ail* (YPO2905) (attachment and invasion of mammalian cells), *katA* (catalase), *katY* (catalase), *fadABDH* (fatty acid degradation), *treBC* (trehalose metabolism), *terZ* (tellurium resistance protein), *metK* (*S*-adenosylmethionine synthetase), *ureABCDEFG*, and *ompW* (putative exported protein), and genes involved in the Krebs cycle. Genes downregulated in response to AI-2 included *rpl* (ribosomal proteins), *yopMP* and *yscBCDEFGHIJKLMS* (type III secretion system), *fabABFJ* (fatty acid biosynthesis), *hmuSTU* (hemin transport), *waaL* (putative O-antigen biosynthesis protein), and *lolCDE* (lipoprotein-releasing system).

Differentiated genes in response to purified AI-2. To decipher the role of AI-2 signaling at mammalian host temperatures, an AI-2 add-in study was performed as described above. The results showed a total of 32 differentially regulated genes at a P value of <0.05 and 9 genes at a P value of <0.01 (see Table S3 in the supplemental material). Upregulated genes in AI-2-treated cells with a fold change of >1.5 included only two genes, YPO4086 (lipoprotein) and *fliH* (flagellar assembly protein). Downregulated genes in AI-2-treated cells included *psaAB* (synthesis of the pH 6 antigen precursor, antigen 4), *mgtB* (Mg^{2+} transport ATPase protein B), *terA* (tellurite resistance protein), *ompC* (outer membrane porin protein C), YPO0276, and *yfiA* (σ^{54} modulation protein involved in broad regulatory functions).

Differentiated genes in response to AI-2 and both AHLs. A three-signal add-in study was performed, and the array results showed a total of 30 differentially regulated genes at a P value of <0.05 and 21 genes at a P value <0.01 (see Table S4 in the supplemental material). Upregulated genes in the 3-signal-treated cells with the highest fold change included *cspA1*, *cspA2*, and *cspB* (cold shock proteins); *ibpB* (heat shock protein); *asnA* (aspartate-ammonia ligase); *gntT* (gluconate permease); *psaE* (regulatory protein); *ompAC* (cell envelope proteins); and *gntT* and *fruAB* (carbohydrate transport). Downregulated genes in the three-signal-treated cells included two membrane proteins, YPO0800 and YPO1499; *iucC* (siderophore biosynthesis protein); and *metE* (5-methyltetrahydropteroyltriglutamate–homocysteine *S*-methyltransferase).

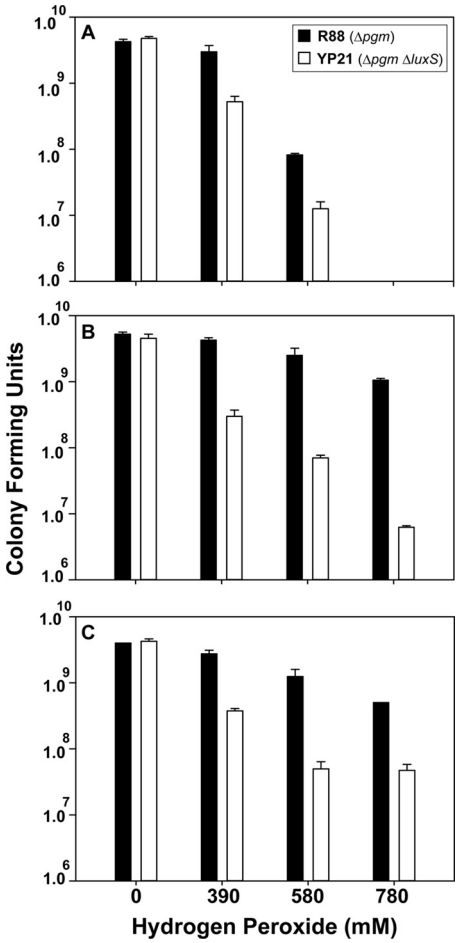

FIG 6 The *Yersinia pestis* Δ*luxS* strain is more sensitive to hydrogen peroxide killing. Strains R88 and YP21 (Δ*luxS* mutant) were grown in BHI broth and exposed to various concentrations of hydrogen peroxide for 1 h. The reactions were quenched, and colony counts were performed. (A) Cells grown at 37°C with supplemented calcium. (B) Cells grown at 30°C with supplemented calcium. (C) Cells grown at 30°C. Data represent the means ± standard deviations of biological triplicates per peroxide concentration tested.

AI-2 is required for resistance to oxidative damage. There are several reports that AI-2 may be important for resistance to oxidative stress in Gram-negative bacteria (22, 23). In addition, our microarray data indicated that a mutation in *luxS* (strain ISM1980) resulted in downregulation of *katY* (see Table S2 in the supplemental material). To assess this phenotype in *Y. pestis*, hydrogen peroxide was used in growth inhibition assays with strain R88 and Δ*luxS* strain YP26. In the presence of the oxidant, YP26 displayed a longer growth lag in culture medium and increased sensitivity on agar plates (data not shown), in accordance with our microarray results (see Table S2 in the supplemental material). To quantify this phenotype, a dose-response curve of peroxide exposure at 37°C (Fig. 6A) and 30°C (Fig. 6B) with calcium and at 30°C without supplementation (Fig. 6C) was performed, and viable

cells were enumerated. Under every condition, the Δ*luxS* mutant displayed increased sensitivity to hydrogen peroxide exposure.

DISCUSSION

In this report, we demonstrate that *Y. pestis* CO92 utilizes an AI-2 QS mechanism that is similar to those of other enteric pathogens. *Yersinia pestis* makes AI-2 in a LuxS-dependent manner during late logarithmic growth, and we identified an *lsr* chromosomal locus that modulates the stationary-phase level of extracellular AI-2. Finally, our findings indicate that AI-2 sensing may be important for resistance to oxidative stress.

A recent study of *Y. pestis* strain KIM demonstrated that *luxS* mutants were unable to make AI-2 and that this phenotype could be complemented (4). Our time course analysis has taken these observations a step further and demonstrated that AI-2 is produced only in a tight window during logarithmic growth (Fig. 1). In stationary phase, the AI-2 levels drop precipitously in an Lsr-dependent manner, similar to what has been observed for *S. enterica* and *E. coli* (6, 18). Whether the concentration decline is due to extracellular degradation of AI-2 or transport is not clear. Considering that the *lsr* locus encodes an LsrACD transporter that is functional in other enteric pathogens (19, 24), it seems likely that the disappearance is due to AI-2 transport.

The results of the AI-2 time course study with the *Y. pestis* Δ*lsr* mutant (Fig. 5) mirror the findings for *S. enterica* and *E. coli* (18, 24). In all three pathogens, when the Lsr transporter is deactivated, the extracellular AI-2 levels are prolonged but eventually drop to lower levels. These observations prompted the proposal that another low-affinity or cryptic AI-2 transporter may exist. The *lsrACDBFGE* operon shows striking parallels to the *rbs* operon (19), which encodes functions required for ribose transport. In the oral pathogen *Actinobacillus actinomycetemcomitans*, the periplasmic ribose receptor RbsB binds AI-2 with strong affinity (12). However, a knockout of the *rbs* system in *A. actinomycetemcomitans* had only a minimal effect on AI-2 extracellular levels (25), paralleling observations made previously with *E. coli* (26). Taken together, the Lsr system is the primary mechanism of AI-2 transport in most bacteria, and the Rbs system functions at a secondary level. Both the *lsr* and *rbs* systems need to be deactivated for maintaining extracellular AI-2 levels (25). Similar to other bacteria, a chromosomal locus with similarity to the *rbs* operon is present in *Y. pestis* CO92 (ORFs YPO3633 to YPO3639), which could be functioning in this capacity. Other transporters, such as the TqsA protein (27), could also be contributing to the stationary-phase drop in AI-2 levels in the Δ*lsr* mutant (Fig. 5), and a TqsA homologue is present on the *Y. pestis* CO92 chromosome (YPO2450). Further investigation is necessary to clarify possible roles of the putative *rsb* locus or TqsA in AI-2 binding and transport.

Our findings with the *Y. pestis* Δ*luxS* mutant demonstrating an increased sensitivity to hydrogen peroxide killing compared to the *luxS*$^+$ control strain (R88) suggest a role for AI-2 in the oxidative stress response. *Yersinia pestis* possesses two functional catalases, KatA and KatY, that are known to contribute to hydrogen peroxide resistance (28). Reduced levels of one or both of these enzymes could explain the increased sensitivity to oxidative stress (Fig. 4). Although subtle temperature regulation of the *katY* gene has been reported (28), we did not observe significant temperature or calcium dependence in our killing assay.

Knockouts of the *luxS* biosynthetic gene in many pathogenic bacteria have revealed broad-spectrum phenotypes. These phenotypic changes can range from biofilm defects to altered expression of virulence factors and have been summarized in review articles (29). While we have identified a putative role for AI-2 signaling during oxidative stress, other studies have linked the system to *Y. pestis* biofilm formation (4), an important factor during growth in the flea. However, the biofilm phenotype was observed in combination with acyl homoserine lactone knockouts, suggesting that the contribution of AI-2 to this phenotype is unclear.

Our studies show that the *Y. pestis* AI-2 quorum-sensing system functions in a manner similar to that in the *S. enterica* paradigm model. Both pathogens make AI-2 during logarithmic growth, modulate extracellular levels by using the Lsr system, and recognize the (2*R*,4*S*)-2-methyl-2,3,3,4-tetrahydroxytetrahydrofuran (*R*-THMF) form of the signal (30). We have gone further and uncovered a function for AI-2 in the *Y. pestis* oxidative stress response, shedding light on a potential role for the system in host interactions. Beyond these enteric pathogens, recent studies with the plant symbiont *Sinorhizobium meliloti* indicate that the Lsr system is also present in nonpathogenic bacteria (21). Interestingly, *S. meliloti* does not possess *luxS* but responds to the *R*-THMF form of exogenous AI-2 by using an Lsr system, providing a new twist on this signaling theme. As the list of bacteria with functional AI-2 systems continues to grow, we are gaining an improved understanding of the contribution of this communication mechanism to the lifestyles of diverse Gram-negative and Gram-positive bacteria.

More than 100 bacteria can produce and detect AI-2 quorum-sensing signals; therefore, AI-2/LuxS quorum sensing is thought to represent an important means of intergeneric communication (31). To clarify the function of AI-2-mediated QS in *Y. pestis*, we compared the transcriptomes of the Δ*pgm* strain of CO92 with mutant QS strains using microarrays. This gave us insight into the role of AI-2 in gene expression on a global basis. According to the number of significantly regulated genes in the microarray experiments in this study (see Table S2 in the supplemental material), AI-2 quorum sensing was an important regulator of gene expression at 37°C, with an effect on 615 genes at a P value of <0.05 and an absolute-value fold change of >1.5 in the Δ*luxS*::*kan* mutant study (strain ISM1980).

Since this experiment involved full induction of both AHL pathways, the AI-2 addition study might better isolate only the AI-2 contribution to gene expression, with a more modest number of 32 significant genes at a P value of <0.05 (see Table S3 in the supplemental material). In this experiment, only AI-2 induction would have been operative since the growth phase was too early for an AHL contribution, as shown in previous studies (13).

In this study, we found numerous metabolism-associated genes, such as those involved with maltose, galactose, arabinose, and fatty acid metabolism, that were downregulated in the Δ*luxS*::*kan* mutant. In support of this, there is evidence that AI-2 QS can regulate carbohydrate metabolism in *Streptococcus gordonii* (32). Bacteria transport maltose and galactose from extracellular fluid into the cytosol. Why is it important? We know that maltose or galactose can be utilized for nutrition, although fatty acids are toxic to *E. coli*. The *malQ* gene, encoding a maltodextrin phosphorylase, is a pseudogene in *Y. pestis*. This mutation prevents glucose-1-phosphate from converting back to glucose to complete the O-antigen unit. We know that *Y. pestis* contains the core constituents of lipopolysaccharide but lacks the extended O-group side chains (33). The *agaYZ* operon is involved in the metabolism

of *N*-acetylgalactosamine and *N*-acetylgalactosamine. Both sugars are concentrated in sensory nerve structures, are components of the interstitial tissues of both humans and animals, and are necessary for intercellular communication. Disruption of host tissues by degradation of these sugars might enhance bacterial spread. The *agaYZ* genes were downregulated in Δ*luxS*::*kan* mutant strain ISM1980 and triple QS mutant strain ISM1185, suggesting that *agaYZ* is under quorum-sensing control.

As a Gram-negative bacterium, *Y. pestis* requires that nutrients pass through outer and inner membranes. Around 84 inner and outer membrane proteins, including lipoproteins and porins, were up- or downregulated in the Δ*luxS*::*kan* mutant. This suggests that remodeling of the cell envelope might be one response when the *luxS* gene is mutated. *yapM* (YPO0823) encodes an autotransporter membrane protein that showed decreased expression levels in Δ*luxS*::*kan* mutant strain ISM1980. These results suggest that *yapM* is regulated by AI-2/LuxS. The function of *yapM* requires further investigation. The gene for the envelope protein OmpW, a putative exported protein with unknown function, was also downregulated in the Δ*luxS*::*kan* mutant.

Oxidative stress is encountered by *Y. pestis* under a variety of conditions by exposure to various highly reactive oxygen derivatives. In response to the *luxS* mutation, the catalase gene *katA* (YPO1207); *katY* (YPO3319), which encodes catalase-peroxidase; and *ahpC* (YPO3194) (alkyl hydroperoxide reductase subunit C) were upregulated in R88 to supposedly help *Y. pestis* combat oxidative stress inside host cells. The *ahpC* gene also has a role in resistance to peroxynitrite and stage-specific survival in macrophages. To support this hypothesis, we showed that a *luxS* mutant was more sensitive to hydrogen peroxide exposure than the control strain (Fig. 6).

The 70-kb virulence plasmid pCD in *Y. pestis* encodes a type III secretion system (TTSS) that injects cytotoxins, termed Yops, into the mammalian cytosol. The TTSS transcripts were upregulated in both strains containing a *luxS* mutation, ISM1980 and R115. Although there is some evidence that LuxS does not affect the expression of the TTSS in *Salmonella* (34), our data show that this does not appear to be the case in *Y. pestis* CO92. Two other virulence-related genes, *psaA* and *mgtB*, were also downregulated in AI-2-treated cells. These results indicate that *luxS* and three QS systems can decrease the expression levels of some virulence factors that may have important consequences for disease. Despite the fact that a KIM5 *luxS* mutant failed to reduce the LD_{50} in a mouse model of virulence (4), other disease parameters and models, i.e., pneumonic disease and tissue specificities, etc., should be studied in light of these new findings.

In this report, we demonstrated that *Y. pestis* CO92 utilizes an AI-2 quorum-sensing mechanism that is similar to those of other enteric pathogens. *Yersinia pestis* makes AI-2 in a LuxS-dependent manner during late logarithmic growth. To study this further, we performed a comparative analysis with a *lsr* chromosomal locus that modulates the stationary-phase level of extracellular AI-2. Our array data indicate that AI-2 QS affects the general physiology of the cell and may impact the expression of virulence factors as well. Finally, our findings indicate that AI-2 sensing may be important for resistance to oxidative stress and membrane modeling during quorum sensing. The consequences of such changes and their impact on disease are not understood and should be studied further.

ACKNOWLEDGMENTS

We thank R. Perry for *Y. pestis* strains R88 and R115 and Carrie Oster and Jenny Boonyakuakel for technical assistance.

This work was supported by Office of Naval Research grant N00014-06-1-1176 to F.C.M., A.R.H, and G.J.P.

REFERENCES

1. **Achtman M, Zurth K, Morelli G, Torrea G, Guiyoule A, Carniel E.** 1999. *Yersinia pestis*, the cause of plague, is a recently emerged clone of *Yersinia pseudotuberculosis*. Proc. Natl. Acad. Sci. U. S. A. **96:**14043–14048.
2. **Ayyadurai S, Houhamdi L, Lepidi H, Nappez C, Raoult D, Drancourt M.** 2008. Long-term persistence of virulent *Yersinia pestis* in soil. Microbiology **154:**2865–2871.
3. **Brubaker RR.** 1983. The Vwa+ virulence factor of yersiniae: the molecular basis of the attendant nutritional requirement for Ca++. Rev. Infect. Dis. **5**(Suppl 4):S748–S758.
4. **Bobrov AG, Bearden SW, Fetherston JD, Khweek AA, Parrish KD, Perry RD.** 2007. Functional quorum sensing systems affect biofilm formation and protein expression in *Yersinia pestis*. Adv. Exp. Med. Biol. **603:**178–191.
5. **Chen X, Schauder S, Potier N, Van Dorsselaer A, Pelczer I, Bassler BL, Hughson FM.** 2002. Structural identification of a bacterial quorum-sensing signal containing boron. Nature **415:**545–549.
6. **Xavier KB, Miller ST, Lu W, Kim JH, Rabinowitz J, Pelczer I, Semmelhack MF, Bassler BL.** 2007. Phosphorylation and processing of the quorum-sensing molecule autoindiucer-2 in enteric bacteria. ACS Chem. Biol. **2:**128–136.
7. **Doll JM, Zeitz PS, Ettestad P, Bucholtz AL, Davis T, Gage K.** 1994. Cat-transmitted fatal pneumonic plague in a person who traveled from Colorado to Arizona. Am. J. Trop. Med. Hyg. **51:**109–114.
8. **Greenberg EP, Hastings JW, Ulitzur S.** 1979. Induction of luciferase synthesis in *Beneckea harveyi* by other marine bacteria. Arch. Microbiol. **120:**87–91.
9. **Datsenko KA, Wanner BL.** 2000. One-step inactivation of chromosomal genes in *Escherichia coli* K-12 using PCR products. Proc. Natl. Acad. Sci. U. S. A. **97:**6640–6645.
10. **Wang J, Sarov M, Rientjes J, Fu J, Hollak H, Kranz H, Xie W, Stewart AF, Zhang Y.** 2006. An improved recombineering approach by adding RecA to lambda Red recombination. Mol. Biotechnol. **32:**43–53.
11. **Schauder S, Shokat K, Surette MG, Bassler BL.** 2001. The LuxS family of bacterial autoinducers: biosynthesis of a novel quorum-sensing signal molecule. Mol. Microbiol. **41:**463–476.
12. **Miller ST, Xavier KB, Campagna SR, Taga ME, Semmelhack MF, Bassler BL, Hughson FM.** 2004. *Salmonella typhimurium* recognizes a chemically distinct form of the bacterial quorum-sensing signal AI-2. Mol. Cell **15:**677–687.
13. **LaRock C, Yu J, Horswill AR, Parsek MR, Minion FC.** 2013. Transcriptome analysis of acyl-homoserine lactone-based quorum sensing regulation in *Yersinia pestis*. PLoS One **8:**e62337. doi:10.1371/journal.pone.0062337.
14. **Carruthers MD, Minion C.** 2009. Transcriptome analysis of *Escherichia coli* O157:H7 EDL933 during heat shock. FEMS Microbiol. Lett. **295:**96–102.
15. **Madsen ML, Nettleton D, Thacker EL, Edwards R, Minion FC.** 2006. Transcriptional profiling of *Mycoplasma hyopneumoniae* during heat shock using microarrays. Infect. Immun. **74:**160–166.
16. **Gallup JM, Ackermann MR.** 2006. Addressing fluorogenic real-time qPCR inhibition using the novel custom Excel file system 'Focusfield2-6GallupqPCRSet-upTool-001' to attain consistently high fidelity qPCR reactions. Biol. Proced. Online **8:**87–152.
17. **Fetherston JD, Schuetze P, Perry RD.** 1992. Loss of the pigmentation phenotype in *Yersinia pestis* is due to the spontaneous deletion of 102 kb of chromosomal DNA which is flanked by a repetitive element. Mol. Microbiol. **6:**2693–2704.
18. **Taga ME, Miller ST, Bassler BL.** 2003. Lsr-mediated transport and processing of AI-2 in *Salmonella typhimurium*. Mol. Microbiol. **50:**1411–1427.
19. **Taga ME, Semmelhack JL, Bassler BL.** 2001. The LuxS-dependent autoinducer AI-2 controls the expression of an ABC transporter that functions in AI-2 uptake in *Salmonella typhimurium*. Mol. Microbiol. **42:**777–793.
20. **Sun J, Daniel R, Wagner-Dèobler I, Zeng AP.** 2004. Is autoinducer-2 a universal signal for interspecies communication: a comparative genomic

and phylogenetic analysis of the synthesis and signal transduction pathways. BMC Evol. Biol. **4:**36. doi:10.1186/1471-2148-4-36.
21. **Pereira CS, MacAuley JR, Taga ME, Xavier KB, Miller ST.** 2008. *Sinorhizobium meliloti*, a bacterium lacking the autoinducer (AI-2) synthase, responds to AI-2 supplied by other bacteria. Mol. Microbiol. **70:** 1223–1235.
22. **He YW, Frye JG, Strobaugh TP, Chen CY.** 2008. Analysis of AI-2/LuxS-dependent transcription in *Campylobacter jejuni* strain 81-176. Foodborne Pathog. Dis. **5:**399–415.
23. **Krin E, Chakroun N, Turlin E, Givaudan A, Gaboriau F, Bonne I, Rousselle JC, Frangeul L, Lacroix C, Hullo MF, Marisa L, Danchin A, Derzelle S.** 2006. Pleiotropic role of quorum-sensing autoinducer 2 in *Photorhabdus luminescens*. Appl. Environ. Microbiol. **72:**6439–6451.
24. **Xavier KB, Bassler BL.** 2005. Regulation of uptake and processing of the quorum-sensing autoinducer AI-2 in *Escherichia coli*. J. Bacteriol. **187:** 238–248.
25. **Shao H, James D, Lamont RJ, Demuth DR.** 2007. Differential interaction of *Aggregatibacter* (*Actinobacillus*) *actinomycetemcomitans* LsrB and RbsB proteins with autoinduer 2. J. Bacteriol. **189:**5559–5565.
26. **Hardie KR, Cooksley C, Green AD, Winzer K.** 2003. Autoinducer 2 activity in *Escherichia coli* culture supernatants can be actively reduced despite maintenance of an active synthase, LuxS. Microbiology **149:**715–728.
27. **Herzberg M, Kaye IK, Peti W, Wood TK.** 2006. YdgG (TqsA) controls biofilm formation in *Escherichia coli* K-12 through autoinducer 2 transport. J. Bacteriol. **188:**587–598.
28. **Han Y, Geng J, Qui Y, Guo Z, Zhou D, Bi Y, Du Z, Song Y, Wang X, Tan Y, Zhu Z, Zhai J, Yang R.** 2008. Physiological and regulatory characterization of KatA and KatY in *Yersinia pestis*. DNA Cell Biol. **27:** 453–462.
29. **Vendeville A, Winzer K, Heurlier K, Tang CM, Hardie KR.** 2005. Making 'sense' of metabolism: autoinducer-2, LuxS and pathogenic bacteria. Nat. Rev. Microbiol. **3:**383–396.
30. **Kavanaugh JS, Gakhar L, Horswill AR.** 2011. The structure of LsrB from *Yersinia pestis* complexed with autoinducer-2. Acta Crystallogr. Sect. F Struct. Biol. Cryst. Commun. **67:**1501–1505.
31. **Xavier KB, Bassler BL.** 2003. LuxS quorum sensing: more than just a numbers game. Curr. Opin. Microbiol. **6:**191–197.
32. **McNab R, Ford SK, El-Sabaeny A, Barbieri B, Cook GS, Lamont RJ.** 2003. LuxS-based signaling in *Streptococcus gordonii*: autoinducer 2 controls carbohydrate metabolism and biofilm formation with *Porphyromonas gingivalis*. J. Bacteriol. **185:**274–284.
33. **Perry RD, Fetherston JD.** 1997. *Yersinia pestis*—etiologic agent of plague. Clin. Microbiol. Rev. **10:**35–66.
34. **Perrett CA, Karavolos MH, Humphrey S, Mastroeni P, Martinez-Argudo I, Spenser H, Bulmer DM, Winzer K, McGhie E, Koronakis V, Williams P, Khan CM, Jepson MA.** 2009. LuxS-based quorum sensing does not affect the ability of *Salmonella enterica* serovar Typhimurium to express the SPI-1 type 3 secretion system, induce membrane ruffles, or invade epithelial cells. J. Bacteriol. **191:**7253–7259.